Predicting the Effect of Mutations on a Genome-Wide Scale

by

Alexey Strokach

A thesis submitted in conformity with the requirements
for the degree of Master of Science
Graduate Department of Computer Science
University of Toronto

Abstract

Predicting the Effect of Mutations on a Genome-Wide Scale

Alexey Strokach
Master of Science
Graduate Department of Computer Science
University of Toronto
2016

Contents

List of Tables

List of Figures

Chapter 1

Introduction

1.1 Background

Recent advances in DNA sequence technology have drastically lowered the cost and improved the accuracy of genome sequencing [1]. This has made exome and whole-genome sequencing a viable and cost-effective tool in both the laboratory and in the clinic to assist with the diagnosis and direct treatment of pediatric conditions [2] and cancers [3], and has led to an enormous growth in the amount of genomic data that is being generated. However, interpreting such genomic data to produce meaningful and actionable results remains a challenge.

In vitro and *in vivo* experiments remain the gold standard in elucidating the effect of mutations. However, evaluating experimentally the effect of all discovered mutants is not feasible. Computational techniques have been developed to predict the effect of different mutations and to prioritize them for experimental validation. Those techniques generally use conservation score describing the likelihood that a particular amino acid being found in the particular position in orthologous proteins.

The most widely-used program for predicting the deleteriousness of a mutation is Sorting Intolerant from Tolerant (SIFT) [4]. SIFT runs PSI-Blast to create a multiple sequence alignment for the query protein, and computes a conservation score by looking at the likelihood of the wildtype and mutant amino acids occurring at a given position in the alignment. While SIFT is a well-established tool in the field, it is difficult to compile and install on a local machine. Furthermore, multiple sequence alignments constructed by SIFT can be several megabytes in size, and caching this data for an entire proteome would require a non-trivial amount of storage space.

Another popular sequence-based algorithm is Provean [5]. Provean also calculates uses PSI-Blast to calculate a multiple sequence alignment. However, it then runs CD-HIT to select under 100 representative sequences capturing the diversity of the alignment, and then performs pairwise alignments with this "supporting set" to predict the final score. Provean is reported to achieve similar performance to SIFT. However, unlike SIFT, it is freely available under the GPLv3 license, it compiles easily and runs on modern Linux distributions. Furthermore, Provean is distributed under a license, and uses *supporting sets* of at most 45 sequences which can be precalculated and stored. If a supporting set is available, calculating the Provean score takes several seconds per mutation.

The performance of Provean is comparable to the leading mutation scoring programs, such as SITF, PolyPhen-2, Mutation Assessor, and CONDEL [5]. Furthermore, Provean is distributed under a GPLv3

license, and uses *supporting sets* of at most 45 sequences which can precalculated and stored. If a supporting set is available, calculating the Provean score takes several seconds per mutation.

Another widely-used mutaiton scoring tool is PolyPhen-2. It is one of the packages predicted for

Many other tools have been developed that offer various advantages over SIFT / Provean. PolyPhen-2 [6] uses support vector machines to combine a conservation score with different sequential and structural features of the wildtype and mutant residue. However, since PolyPhen-2 is trained on a dataset of human deleterious mutations, it is difficult to use in downstream applications, as one would have to make sure to exclude the PolyPhen-2 training set throughout the training and validation process. FATHMM [7] constructs a hidden Markov model based on the alignment, and is reported to achieve marginally higher accuracy than SIFT / Provean. Other techniques offering various advantages over SIFT / Provean include MutPred [8], MutationAssesor [9], CADD [10], CONDEL [5], and others.

Despite the proliferation of tools predicting the deleteriousness of different SNPs, our ability to act on those predictions remains limited. Existing computational methods are limited in their accuracy and the type of information that they can provide. Most existing tools use a conservation score. While millions of single nucleotide polymorphisms (SNPs) have been implicated in thousands of diseases, approaches for predicting the phenotypic effect of newly-discovered mutations are still in their infancy. One of the reasons is that while sequence-based tools achieve reasonably good performance at predicting whether or not a given mutation is going to be deleterious, they fall short in predicting *why* that mutation is deleterious. This lack of actionable predictions limits the usability of the vast DNA sequencing data that has been generated. However, the etiology by which the mutations cause or contribute to a disease are often unknown.

- Existing approaches remain limited in their ability to predict disease-causing variants. In a study of 1571 mutations of the CFTR gene causing cystic fibrosis, (SIFT, PolyPhen, PANTHER) [11]

1.2 Structural approaches to predicting the effect of mutations

Statistical potentials

Physics-based methods the electrostatic, van der Waals, solvent accessible surface area, and entropy terms

Concoord/Poisson-Boltzmann surface area (CC/PBSA server)

The central dogma of biology is that DNA is transcribed into RNA which is translated into Protein.

One reason for out lack of ability in interpreting is the focus on the sequence-level features, while in the majority of missense mutations, it is the alteration in the function of the transcribed protein which is responsible for the detrimental effect of mutations.

The field of protein science has generally been concerned with the broad questions of protein folding, protein design. Algorithms have been developed to predict the effect of mutations on protein folding and protein-protein affinity, but those tools are generally meant to be used on a case-by-case basis and have not been designed to be applied on a genome-wide scale to predict the effect of missense mutations from whole-genome sequencing studies.

While the growth in protein crystal structures has not seen the rapid rise that was observed in DNA sequencing, the number of resolved protein structures has also been increasing, with the Protein Data Bank (PDB) containing close to 125,000 structures as of 2016.

A related are of research is predicting the energetic effect of mutations.

The most accurate class of computational techniques are alchemical free energy calculations, which involve modelling the structural transition from the wildtype to the mutant protein and using the Bennett acceptance ratio (BAR) or thermodynamic integration (TI) to calculate the energetics of the transition [12]. However, alchemical free energy calculations are computationally expansive, and are generally used only in cases where the experimental characterization of mutants is particularly difficult, as in the case of D-amino acid peptide design [13].

Many algorithms have been developed which attempt to predict the effect of mutations on protein stability and / or on protein-protein interaction affinity. Those techniques generally use a rigid backbone representation of protein and use statistical potentials. For a review see XXX.

Mixed strategies which utilize both sequence- and structure-based approaches. Such algorithms include PoPMuSiC,

Structure-based tools which predict the effect of mutations on protein structure and / or function using features describing the three-dimensional structure of the protein. mCSM [14] (graph-based signatures), MAESTRO [15] (multi-agent machine learning), CC/PBSA (Concoord/Poisson-Boltzmann surface area) [16],

Some algorithms rely on the conservation of the residue in multiple sequence alignments.

Predicting protein thermal stability changes upon point mutations using statistical potentials: Introducing HoTMuSiC

- MAESTRO implements a multi-agent machine learning system.

- Structure based tools AUTO-MUTE [7], CUPSAT [8], Dmutant [9], FoldX [10], Eris [11], PoPMuSiC [12], SDM [13] or mCSM [14] usually perform better than the sequence based counterparts. Recently, SDM and mCSM have been integrated into a new method called DUET [15].

INPS: predicting the impact of non-synonymous variations on protein stability from sequence

- `http://bioinformatics.oxfordjournals.org/content/31/17/2816.long`

- Here, we describe INPS, a novel approach for annotating the effect of non-synonymous mutations on the protein stability from its sequence.

- [17]

FoldX

PoPMuSiC

RosettaCM

mCSM: predicting the effects of mutations in proteins using graph-based signatures.

- `http://www.ncbi.nlm.nih.gov/pubmed/24281696`

- "To understand the roles of mutations in disease, we have evaluated their impacts not only on protein stability but also on protein-protein and protein-nucleic acid interactions".

- [14]

Predicting Binding Free Energy Change Caused by Point Mutations with Knowledge-Modified MM/PBSA Method

- `http://journals.plos.org/ploscompbiol/article?id=10.1371%2Fjournal.pcbi.1004276`

- "The core of the SAAMBE method is a modified molecular mechanics Poisson-Boltzmann Surface Area (MM/PBSA) method with residue specific dielectric constant".

- [18]

Rosetta benchmark [19]

Benchmark showing Rosetta doing poorly: [20]

I-Mutant2, DMutant, CUPSAT, FoldX [21]

1.3 Goals and objectives

- Evaluate how well we can predict the deleteriousness of a mutation by measuring the effect of protein folding on protein stability.
- Assessing the impact of missense mutations.
- Protein engineering. For example generating biological therapeutics that are more thermostable and have a higher affinity for their target.
- Basic science: characterizing the forces that are most important in protein folding and binding, and the effect of mutations on those forces.
- In this work we examine how much sequence-based features can aid in the prediction of traditionally structural realms such as the prediction of $\Delta\Delta G$ scores of mutations, and how much structure-based features can aid with the prediction of mutation pathogenicity–a traditionally sequence based

1.4 Acknowledgements

This is a continuation of the work performed by Niklas Berliner *et al.* [22]. In 2 we discuss how we expand ELASPIC to work on the genome-wide scale. In 3 we discuss how we retrained ELASPIC while leveraging the information we extracted from genome-wide analysis.

Chapter 2

Implementation

2.1 Profs

ELASPIC uses a domain-based approach for creating homology models of query proteins, and therefore requires access to accurate domain definitions. The most widely-used source of protein domain definitions is Pfam [23]. However, since Pfam domains definitions are based entirely on protein sequence, they correlate poorly with the structural fold of the protein. Using Pfam domain definitions when making homology models tends to produce unstable models of fragmented and / or truncated domains, and this would compromise our subsequent analysis of the structural impact of mutations.

In order to improve the structural accuracy of Pfam domains, Andres Felipe Giraldo Forero developed a pipeline that uses structural alignments and a set of heuristics to modify Pfam domain definitions and make them better aligned with the tertiary structure of the protein, as defined by CATH [24]. He named this pipeline Profs, for Protein families. A schematic of this pipeline is presented in Figure 2.1, and the R package implementing the pipeline is available at `https://bitbucket.org/afgiraldofo/profs`. Profs domains have an advantage over Pfam domains in that they have been corrected and expanded to match the structural fold of the protein. They also have an advantage over CATH domains in that they are backed by large, manually-seeded alignments, and can be easily detected in any protein sequence using Pfam HMMs.

We used Andres' pipeline to annotate with Profs domains all proteins in the UniProt database. The resulting table of Profs domain definitions is available for download from the ELASPIC website (`http://elaspic.kimlab.org/static/download/`) and is included in the ELASPIC database (see **domain** and **domain_contact** tables in Figure 2.6 and Table 2.1). The following sections describe the procedure used to generate lists of Profs domain definitions and Profs domain-domain interactions that are used by ELASPIC.

2.1.1 Domains

We used Profs domain definitions calculated, as part of the Profs pipeline, for all proteins in the PDB, to find Profs domains, and structural templates for those domains, for all proteins in Uniprot. To do this, we followed a similar process to what was done to annotate with Profs domains structures in the PDB that lack CATH annotations [25].

We started with Pfam domain definitions for all known protein sequences, which we download from

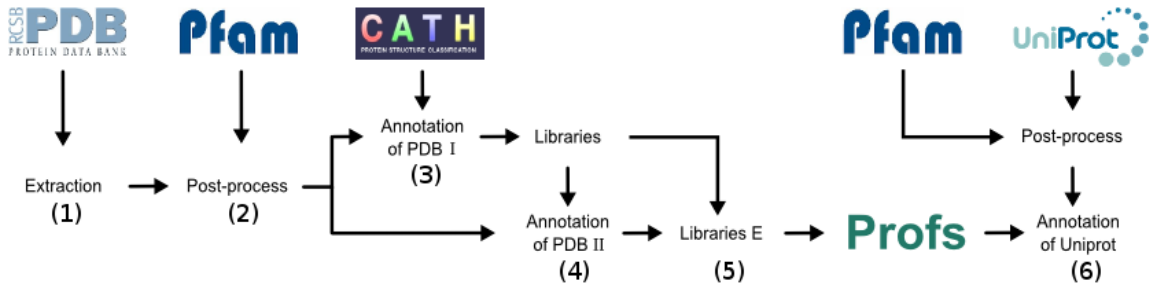

Figure 2.1: Flowchart illustrating steps in the Profs pipeline (courtesy of Andres Felipe Giraldo Forero). Each step in the flowchart is annotated with the section number where that step is explained. **(1)** All structures in the PDB are parsed to extract protein sequences, and HMMScan is ran to find Pfam domains in those sequences. **(2)** Pfam domains of proteins in the PDB are processed in order to join and / or remove overlapping and repeating domains. **(3)** Pfam domain definitions are altered in order to make them compatible with CATH definitions, for structures that have been annotated by CATH. **(4)** Pfam domain definitions are altered in order to make them compatible with CATH definitions, for structures that have not been annotated by CATH. This is done by performing pairwise alignments with structures that do have CATH annotations. **(5)** Libraries of Profs domain definitions, and Profs domain-domain interactions, are generated for all proteins in the PDB. **(6)** Libraries of Profs domain definitions, and Profs domain-domain interactions, are generated for all proteins in Uniprot.

the SIMAP website [26]. We mapped those protein sequences to Uniprot using the MD5 hash of each sequence, and we joined or removed overlapping and repeating domains using a mapping table supplied with the Profs R package. Next, we tried to find a Profs structural template for each Pfam domain by running *blastp* against libraries of Profs domains, which are included in the Profs R package. If a suitable template was found, we proceeded to do iterative global alignments using Muscle [27] while expanding domain boundaries of the Pfam domains to match domain boundaries of the Profs templates. If two Pfam domains were expanded to occupy the same region in the protein, that region was divided in equal parts to the preceding and the succeeding domains.

The results of this analysis are stored in the **uniprot_domain** and the **uniprot_domain_template** tables in the ELASPIC database (Figure 2.6). The **uniprot_domain** table contains all Pfam domains and supradomains that were obtained after removing repeating and overlapping domains, as outlined above. The *pdbfam_name* column contains the name of the Profs domain. The *alignment_def* column contains either the original Pfam domain definitions or, in the case of supradomains, the merged domain definitions of multiple Pfam domains. The **uniprot_domain_template** table contains information describing the alignment of the Pfam domain or supradomain with the corresponding Profs structural template, for domains for which a suitable Profs template could be found. The *cath_id* column identifies the Profs structural template that was selected, and the *domain_def* column contains the corrected and expanded domain definitions.

2.1.2 Comparison with Pfam and Gene3D

In order to ascertain the validity of Profs domain definitions, we compared Profs, Pfam and Gene3D in terms of sequence coverage (Figure 2.2) and domain size (Figure 2.3).

We downloaded Pfam and Gene3D domain definitions for all human proteins from SIMAP [26],

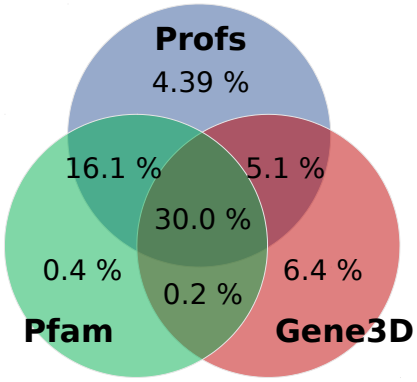

Figure 2.2: Venn diagram showing the overlap in domain definitions between Profs, Pfam, and Gene3D. Values represent the fraction of amino acids, of all human proteins in UniProt, which are covered the particular domain or domains. A total of 18,828 human proteins and 10,868,810 amino acids were considered, after excluding proteins which had no predicted domains by any method. Profs has the highest coverage, with 55.7 % of amino acids being annotated by a Prof domain.

and we calculated Profs domain definitions following the pipeline described above. The analysis was restricted to 18,828 human proteins from UniProt which are annotated with at least one Profs, Pfam or Gene3D domain.

In order to compare sequence coverage, we looked at the fraction of all protein sequences which are covered by each domain type (Figure 2.2). Overall, Profs has the highest sequence coverage, with 55.7 % of 10,868,810 amino acids in 18,828 proteins residing inside a Profs domain. Profs annotates 9 % more amino acids than Pfam and 14 % more amino acids than Gene3D, although the relatively low coverage by Gene3D is expected, as it can only detect domains which are represented in the PDB.

In order to compare domain size, we looked at the average number of domains per protein for each of the three methods (Figure 2.3). Profs has more proteins with only one domain per protein, while Pfam and Gene3D have more proteins with two or more domains per protein. This is consistent with Profs trying to join fragmented and repeating domains into consistent structural units. Gene3D does not detect domains in many proteins with Profs and Pfam domains, likely because those domains have not been crystallized.

The result of this analysis shows that, at least for human proteins, Profs achieves higher sequence coverage using fewer domains per protein than either Pfam or Gene3D. This makes Profs well-suited for the ELASPIC pipeline.

2.1.3 Domain interactions

We also created a table of domain-domain interactions for proteins that are known to interact and for which a homology model of the interaction can be created. We started by creating a comprehensive list of protein-protein interactions (PPIs), by taking the union of all PPIs listed in the HIPPIE database [28] and in the datasets hosted by the Harvard Center for Cancer Systems Biology (CCSB) [29]. The overlap in the PPIs obtained from each source is presented in Figure 2.4. We filtered those PPIs to select pairs of proteins where each protein has at least one domain with a structural template. This information

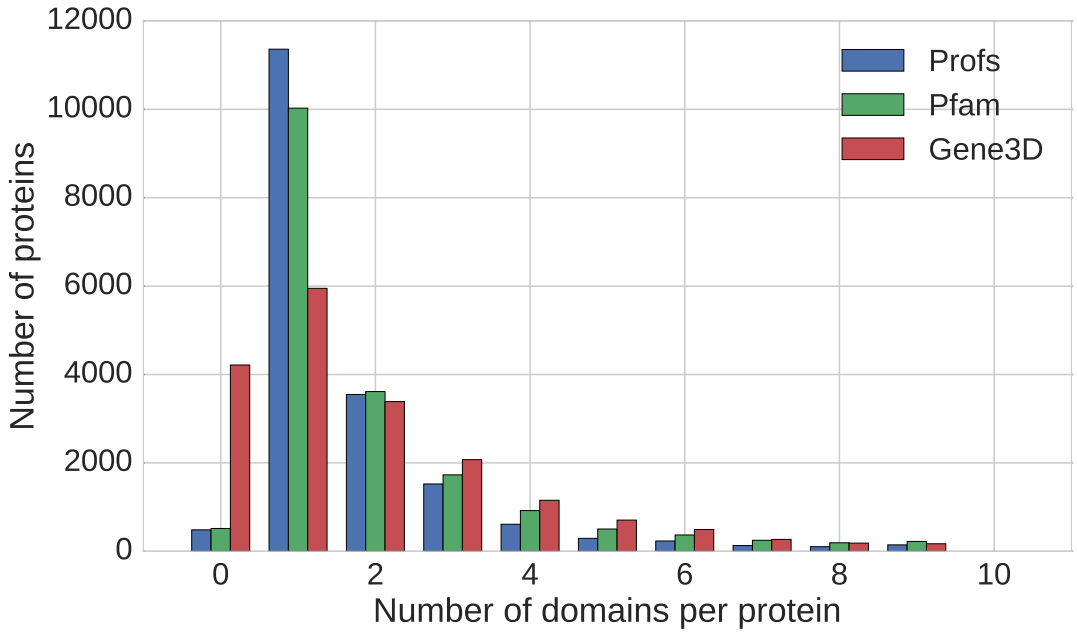

Figure 2.3: Average number of Profs, Pfam and Gene3D domains per protein, for all human proteins containing at least one domains. Profs tends to have fewer domains per protein then either Pfam or Gene3D. Gene3D lacks domain annotation for many proteins which contain at least one Pfam and Profs domain.

is stored in the **uniprot_domain_pair** table. For each of those domains, we perform a Blast search of the domain sequence against a library of Profs domains in the PDB (the **domain** table in Figure 2.6), and we selected only those templates that occur in the same crystal structure in both proteins and that interact according to the **domain_contact** table. In order to select the best template for the interaction, we calculate a quality score for each of the two domains using Equation 2.1, and chose the template with the highest geometric mean of the two scores.

$$alignment\_score = 0.95 \cdot seq\_identity \cdot coverage + 0.05 \cdot coverage \tag{2.1}$$

$$combined\_alignment\_score = \sqrt{alignment\_score\_1 \cdot alignment\_score\_2} \tag{2.2}$$

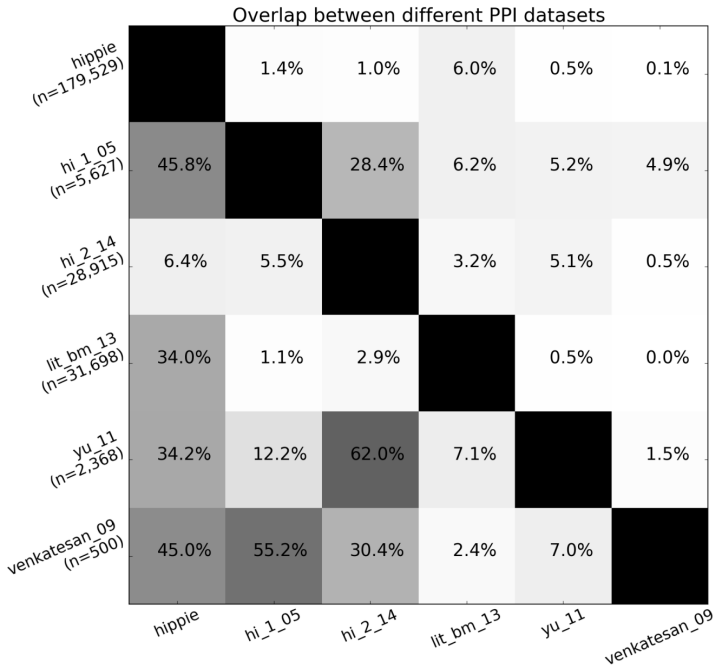

Figure 2.4: Overlap in protein-protein interaction (PPI) databases. The shade and value of each square denotes the percentage of PPIs in the database named on the y-axis that are also found in the database named on the x-axis. **hippie** is a meta-database, which integrates PPIs from many different sources [28]. **hi_1_05** contains PPIs discovered through a proteome-wide yeast two-hybrid experiment conducted by Rual *et al.* [30]. **hi_2_14** contains PPIs discovered through a proteome-wide yeast two-hybrid experiment conducted by Rolland *et al.* [29]. **lit_bm_13** contains PPIs obtained from the literature and supported by multiple pieces of evidence [29]. **yu_11** contains PPIs obtained using "stitch-seq", which combines PCR stitching with next-generation sequencing [31]. **venkatesan_09** corresponds to high-quality binary interactions found in repeat yeast two-hybrid assays conducted by Venkatesan *et al.* [32].

2.2 ELASPIC

The ELASPIC project was started by Niklas Berliner and others in 2014 [22].

ELASPIC uses Modeller [33] to construct homology models of domains and domain-domain interactions, FoldX to optimize those model and to introduce mutations [34], and the GradientBoostingRegressor from scikit-learn [35] to combine FoldX energy scores with sequence-based and other features and predict the energetic impact of a mutation on the stability of a single domain or the affinity between two domains. An overview of the ELASPIC pipeline is presented in Figure 2.5. ELASPIC includes a library Python scripts for construction sequence alignments, constructing Provean supporting sets and computing the Provean score, constructing homology models, running FoldX, and predicting the $\Delta\Delta G$ of the mutation. It also includes a "Standalone Pipeline" (Figure 2.5 right) and a "Database Pipeline" (Figure 2.5 left), which include command line options for mutating a protein structure.

2.2.1 Standalone pipeline

The standalone pipeline works without downloading and installing a local copy of the ELASPIC and PDB databases, but requires a PDB structure or template to be provided for every protein. Pipeline output is saves as JSON files inside the working directory, rather than being uploaded to the database as in the case of the database pipeline. The general overview of the local pipleine is presented in the figure to the right.

The local pipeline still requires a local copy of the Blast nr database.

We used the MODELLER software package to perform all homology modeling.

"MODELLER uses simulated annealing cycles along with a minimal forcefield and spatial restraints – generally Gaussian interatomic probability densities extracted from the template structure with database-derived statistics determining the distribution widthto rapidly generate candidate structures of the target sequence from the provided template sequence."

2.2.2 Database pipeline

The database pipeline allows mutations to be performed on a proteome-wide scale, without having to specify a structural template for each protein. This pipeline requires a local copy of ELASPIC domain definitions and templates, as well as a local copy of the BLAST and PDB databases.

The general overview of the database pipleine is presented in 2.5 left. A user runs the ELASPIC pipeline specifying the Uniprot ID of the protein being mutated, and one or more mutations affecting that protein. At each decision node, the pipeline queries the database to check whether or not the required information has been previously calculated. If the required data has not been calculated, the pipeline calculates it on the fly and stores the results in the database for later retrieval. The pipeline proceeds until homology models of all domains in the protein, and all domain-domain interactions involving the protein, have been calculated, and the $\Delta\Delta G$ has been predicted for every specified mutation.

At each step in the pipeline, a local database is queried to see if the required information has already been calculated. If the information is available, the pipeline moves to the next step. If the information is not available, the pipeline runs the module that generates the required information, stores the generated information in the database for future access, and then moves to the next step. If the specified mutation falls outside of every domain in the protein, no predictions are returned. Otherwise, the pipeline evaluates the impact of the mutation on the stability of the domain and, if the mutation falls in a domain interface,

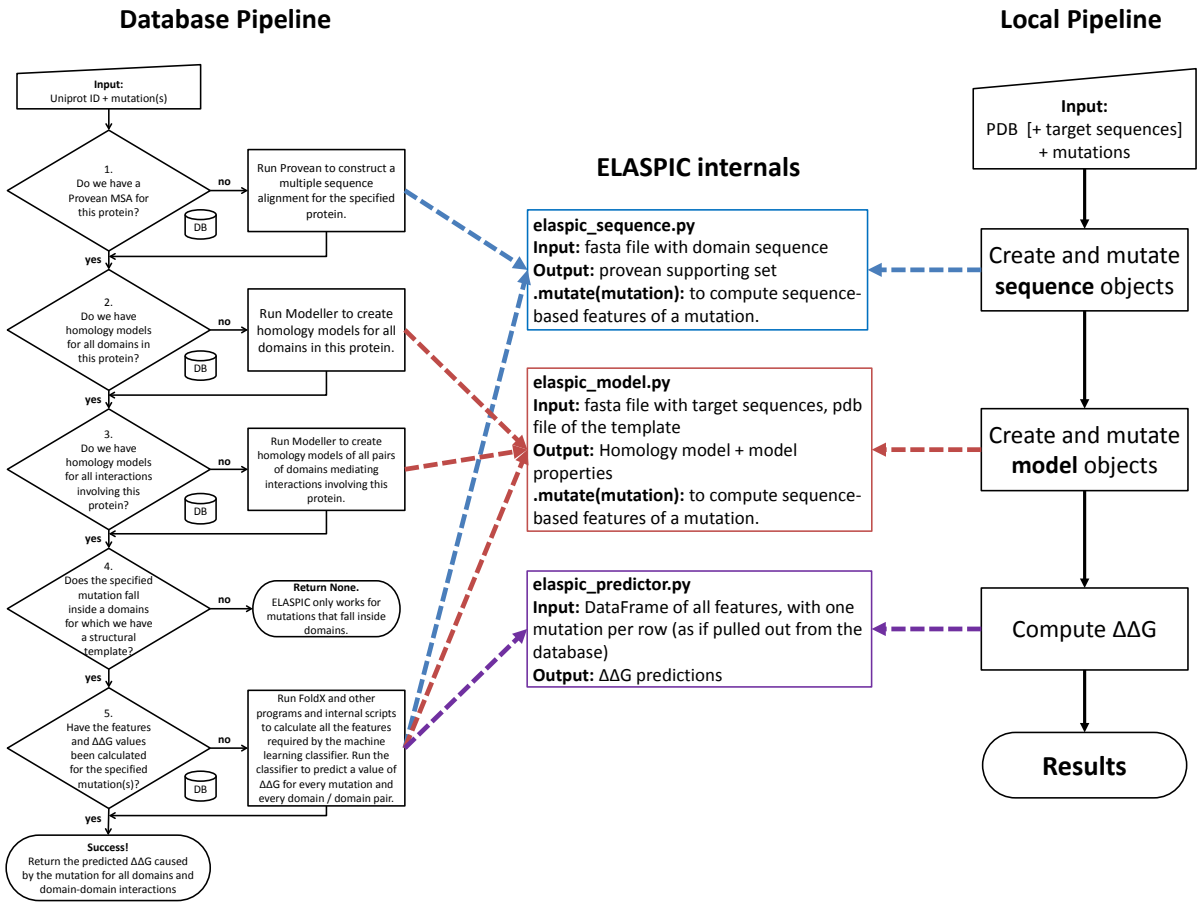

Figure 2.5: Overview of the ELASPIC pipeline. **Database Pipeline:** A user runs the ELASPIC pipeline specifying the UniProt identifier of the protein being mutated, and one or more mutations affecting that protein. At each decision node, the pipeline queries the database to check whether or not the required information has been calculated previously. If the required data has not been calculated, the pipeline calculates it on the fly and stores the results in the database for later retrieval. The pipeline proceeds until homology models of all domains in the protein, and all domain-domain interactions involving the protein, have been calculated, and the $\Delta\Delta G$ has been predicted for every specified mutation. **Local Pipeline:** A user runs the ELASPIC pipeline by specifying the filename of the PDB that they wish to mutate and one or more mutations, or a filename specifying the sequence of the protein that they wish to model, the filename of the PDB that they wish to use as a template, and one or more mutations. ELASPIC runs Provean to calculate the supporting set, runs MODELLER to make the homology model, and runs FoldX to compute structural features describing the wildtype and mutant residues. Results are stored in a local *.elaspic* folder and are not recalculated if the user decides to run more mutations.

on the affinity between two domains. In order to expedite the evaluation of mutations, we precalculated homology models and Provean supporting sets for all human proteins. Structural and sequential features, and predicted $\Delta\Delta G$ scores, have also been precalculated for the majority of mutations listed in the Uniprot humsavar file [36] and in the COSMIC [37] and ClinVar [38] databases.

Provean supporting sets, homology models and mutation $\Delta\Delta G$ scores are available from the ELASPIC downloads page: `http://elaspic.kimlab.org/static/download/`. The source code of the python package implementing the ELASPIC pipeline is available from `https://github.com/kimlaborg/elaspic`, and the documentation for the ELASPIC pipeline can be accessed online at `http://elaspic.readthedocs.`

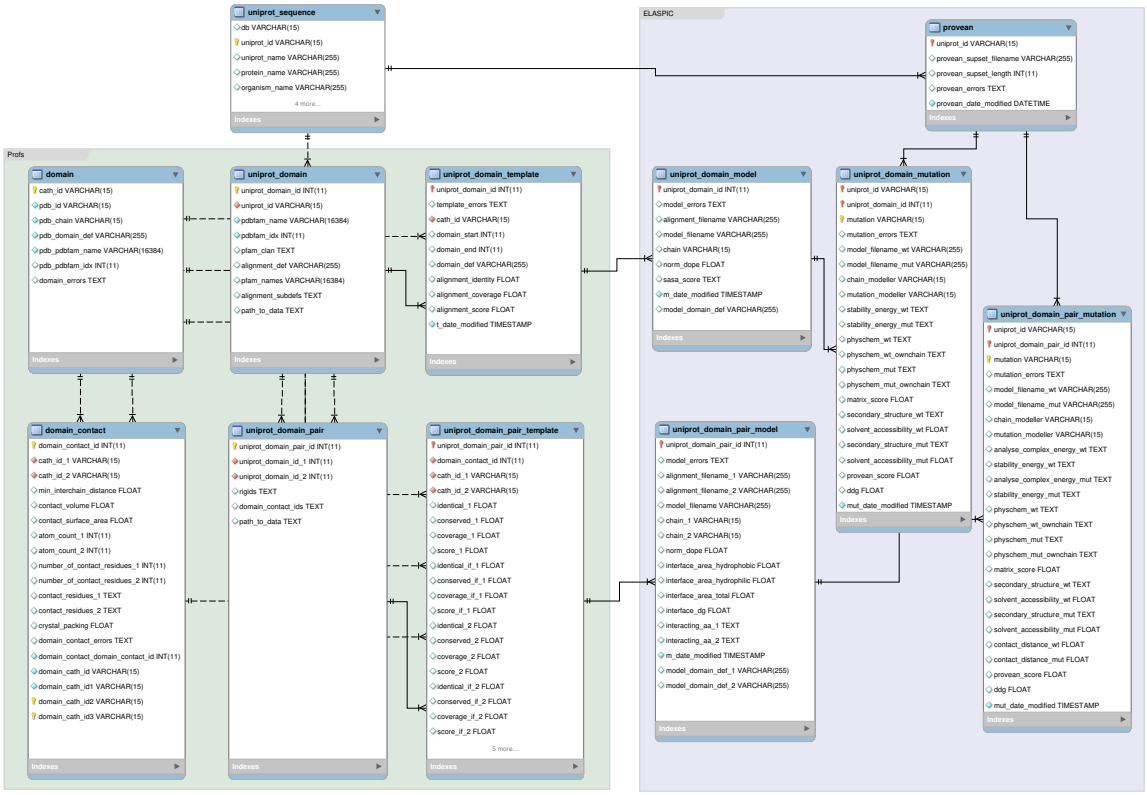

Figure 2.6: ELASPIC database schema. Tables on the green plate titled Profs are calculated using the Profs pipeline, as described in [25]. Tables on the purple plate titled ELASPIC are calculated using the ELASPIC pipeline, following the procedure outlined in 2.5. A detailed description of each table can be found in 2.1.

`org/`.

An overview of the ELASPIC database schema is presented in Figure 2.6, and a description of each database table is provided in Table 2.1.

In the ELASPIC database (Figure 2.6), Profs domain definitions produced by Andres' pipleine are contained in the **domain** and **domain_contact** tables, while Profs domain definitions for uniprot are contained in the **uniprot_domain**, **uniprot_domain_template**, **uniprot_domain_pair**, and **uniprot_domain_pair_template** tables.

Table 2.1: ELASPIC database schema.

Table name	Table description
domain	Contains Profs domain definitions for all proteins in the PDB.
domain_contact	Contains information about interactions between Profs domains in the PDB. Only interactions that are predicted to be real by NOXclass [39] are included in this table.
uniprot_sequence	Contains protein sequences for all proteins that are annotated with Profs domains in the **uniprot_domain** table. This table is constructed by downloading and parsing *uniprot_sprot_fasta.gz*, *uniprot_trembl_fasta.gz* and *homo_sapiens_variation.txt* files from the Uniprot.
provean	Contains information about Provean [5] supporting set files. The construction of a supporting set is the longest part of running Provean. Thus, in order to speed up the evaluation of mutations, the supporting set is precalculated and stored for every protein.
uniprot_domain	Contains Profs domain definitions for proteins in the **uniprot_sequence** table. This table is obtained by downloading Pfam domain definitions for all known proteins from SIMAP [26], and mapping those proteins to Uniprot using the MD5 hash of each sequence. Overlapping and repeating domains are either merged or deleted, as described in [25].
uniprot_domain_template	Contains structural templates for domains in the **uniprot_domain** table. The *domain_def* column contains expanded and corrected domain definitions for every domain.
uniprot_domain_model	Contains information about the homology models that were created using structural templates in the **uniprot_domain_template** table.
uniprot_domain_mutation	Contains information about the structural impact of core mutations, calculated by introducing those mutations into homology models listed in the **uniprot_domain_model** table. The *ddg* column contains the predicted change in the Gibbs free energy of protein folding.
uniprot_domain_pair	Contains pairs of domains that are likely to mediate the interaction between pairs of proteins listed in Hippie [28] and Rolland *et al.* [29].
uniprot_domain_pair_template	Contains structural templates for domain pairs in the **uniprot_domain_pair** table.
uniprot_domain_pair_model	Contains information about homology models that were created using structural templates in the **uniprot_domain_pair** table.
uniprot_domain_pair	Contains information about the structural impact of interface mutations, calculated by introducing those mutations into homology models listed in the **uniprot_domain_pair_model** table. The *ddg* column contains the predicted change in the Gibbs free energy of protein-protein binding.

2.2.3 Jobsubmitter

In order to make ELASPIC accessible to a wider scientific audience, Daniel Witvliet created the ELASPIC webserver, which allows users to run ELASPIC for their protein and mutation of interest and to analyze interactively ELASPIC results [25].

One limitation of the webserver was that it spawned ELASPIC jobs on the same virtual machine as the webserver. This meant that only a few mutations could be analyzed at a time, and that the webserver could stall when running mutations in a protein lacking a precalculated Provean supporting set, since constructing a Provean supporting set could require more RAM than the virtual machine had available. In order to make the webserver scale to thousands of mutations, we attempted to restructure it to run ELASPIC jobs on the lab Sun Grid Engine (SGE) cluster. However, this design introduced several challenges.

First, since users can run multiple mutations affecting the same protein, we had to make sure that the Provean supporting sets and homology models are calculated first, before jobs for individual mutations are submitted to the cluster. Otherwise, each mutation would initiate the calculation of a Provean supporting set, which can require more than 5 GB of memory, and a homology model, which can take more than 30 minutes to complete. This would lead to many unnecessary jobs, drastically lowering our throughput, and could lead to inconsistent results, since different jobs can generate different supporting sets and homology models, even for the same protein, due to the inherent randomness of those tasks.

Second, jobs running on a SGE cluster can die unexpectedly, if, for example, they exceed allocated resources, or if the node on which they are executing experiences a hardware failure. In most cases, the jobs do not get an opportunity to send an error message before they are terminated. Therefore, we had to keep track of all running jobs, and resubmit jobs that do not finish successfully.

Third, in order to send a "Job Complete" email once all mutations submitted by a particular user have been evaluated, we had to keep track of the relationship between mutations and the users that submitted those mutations.

One possible way to address those design requirements would be to use an asynchronous task queue, such as Celery. However, since different tasks inside the queue do not have a shared memory state, each task would have to periodically execute a *qstat* command on the SGE master node in order to monitor the status of the submitted job. Since we could have thousands of mutations running on the cluster at the same time, this would not be a scalable solution.

An alternative approach, which we used for the final design, was to create an independent webservice responsible for submitting ELASPIC jobs to the SGE cluster and monitoring their progress. We called this webservice the ELASPIC "jobsubmitter". It was implemented using the *aiohttp* library, which leverages the *asyncio* event loop and improved support for asyncronous programming present in Python 3.5.

A schematic of the ELASPIC jobsubmitter is presented in Figure 2.7a. Once the jobsubmitter receives a *GET* or *POST* request containing a set of mutations, information concerning those mutations is distributed into the following queues:

- A "Provean" queue, which contains proteins for which a Provean supporting set has not been calculated.
- A "homology model" queue, which contains proteins for which a homology model has not been calculated.

- A "mutation" queue, which contains individual mutations.
- An "email" queue, which contains the set of mutations associated with each job.

The information from those queues is then processed by the corresponding coroutines:

- For each protein in the "Provean" queue, a job is submitted to the SGE cluster, which calculates the Provean supporting set. If the Provean supporting set for the protein has already been calculated, the protein is taken of the "Provean" queue with no further action.
- For each protein in the "homology model" queue, a job is submitted to the SGE cluster, which calculates the homology model of the protein. If the homology model of the protein has already been calculated, the protein is taken of the "homology model" queue with no further action.
- For each mutation in the "mutation" queue, a job is submitted to the SGE cluster, which runs ELASPIC to calculate the $\Delta\Delta G$ of the mutation. This happens *only if the Provean supporting set and homology model for the protein have already been calculated!*
- For each job in the "email" queue, a "Job Complete" email is sent to the specified email address once all mutations for the associated job have been completed.

The ELASPIC jobsubmitter is highly performant. It is able to handle over 150 requests per second, even with 30,000 mutations already being processed by the webservice (Figure 2.7b).

2.3 Precalculated data

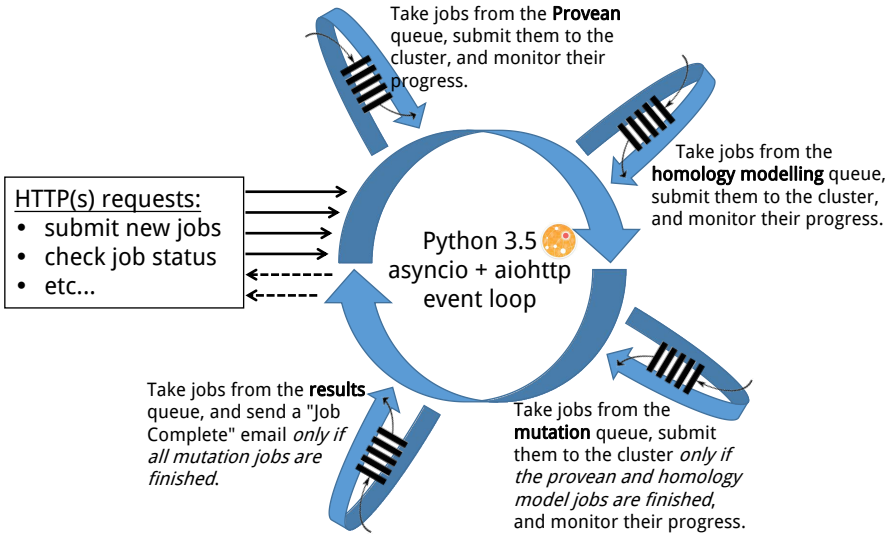

(a) The ELASPIC jobsubmitter was implemented using Python 3.5 and the *aiohttp* library. It includes the *asyncio* event loop, data structures containing information about the mutations being processed, and coroutines which are registered with the *aiohttp* even loop and take turns in performing specific tasks, as described in the figure.

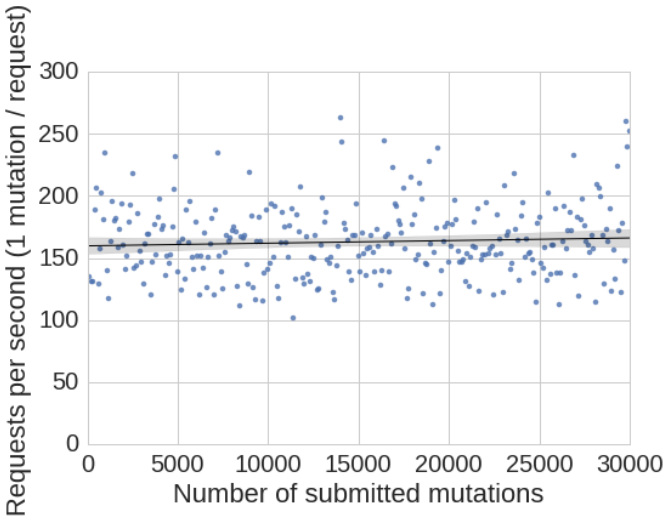

(b) Plot showing the number of requests per second that the ELASPIC jobsubmitter handle, as a function of the number of mutations that are already being processed by the webservice.

Figure 2.7: Implementation (a) and performance (b) of the ELASPIC jobsubmitter.

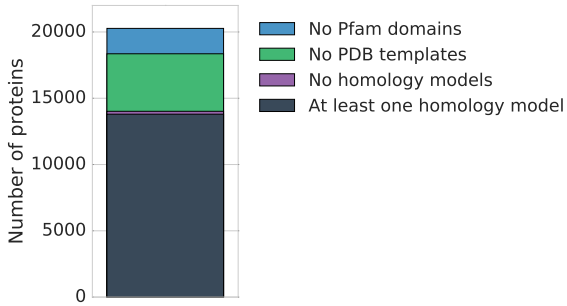

(a) Diagram showing the number of *proteins* in the human SwissProt database that have no Pfam domains (blue), that have Pfam domains but no structural templates (green), that have Pfam domains and structural templates but no homology models (purple), and proteins with a homology model of at least one domain (grey).

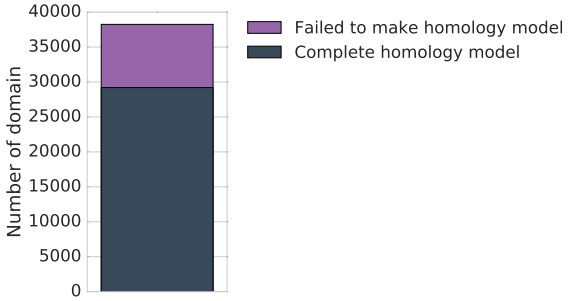

(b) Diagram showing the number of *domains* in all proteins in the human SwissProt database for which we failed to create a homology model (purple) and for which we successfully created a homology model (grey). The most common reason for failing to create a homology model is low sequence identity between the Profs domain and the structural template.

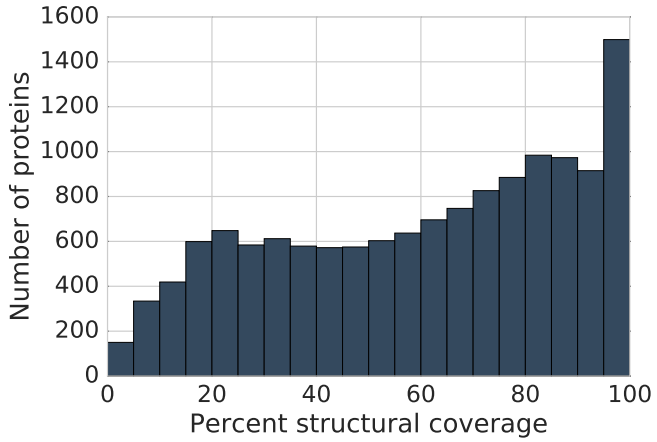

(c) The fraction of protein sequence covered by a Profs domain with a homology model, for all proteins in the human SwissProt database with a homology model of at least one domain.

Figure 2.8: Plots showing the number of proteins for which we could create a homology model (a), the number of domains for which we could create a homology model (b), and the structural coverage of proteins with at least one modelled domain (c). Plots were generated for human proteins in the SwissProt database.

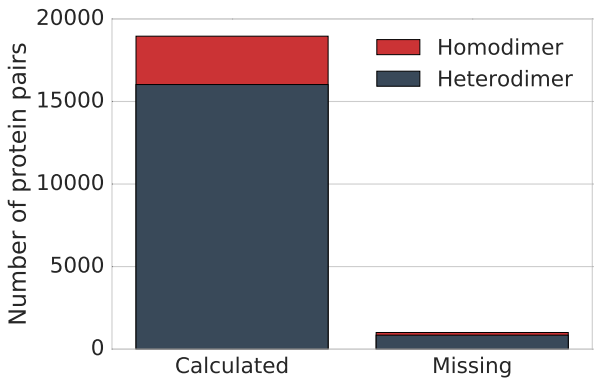

Figure 2.9: Number of homo-dimeric (red) and hetero-dimeric (grey) protein-protein interactions for which we created a homology model (left) and failed to create a homology model (right). In this figure, protein-protein interactions are all pairs of proteins from the human SwissProt database that are found to interact according to one of the protein-protein interaction databases (see Figure 2.4) and that that have at least one structural template of the interaction.

Chapter 3

Results

After making changes to the ELASPIC pipeline that are described in Chapter 2, we retrained ELASPIC core and interface predictors and validated them on new data.

3.1 Datasets

The datasets that were used to train, validate and test the predictors are described in Table 3.1. We made sure that no mutations in the test set appear in our training and validation sets (see Figures 3.1 and 3.2 for core and interface mutations, respectively). In the case of Humsavar, ClinVar and COSMIC datasets, we made sure that no *protein* in the test set appear in the training and validation sets.

Previously, we had seen a low correlation between ELASPIC-predicted $\Delta\Delta G$ and the deleteriousness of mutations. To address this, we split the Humsavar, ClinVar, and COSMIC datasets into validation and test subsets, and used the performance on the validation subset as part of the scoring function for selecting the optimal hyperparameters and number of features.

3.2 Hyperparameter optimisation

We used the $combined\_score_{core}$ and $combined\_score_{interface}$ metrics, given by Equations 3.1 and 3.2, respectively, to evaluate the performance of the predictors during hyperparameter optimization and feature elimination. We expected that this would allow us to select a predictor that performs well not only on the training set, but also generalized to other datasets. While mutation deleteriousness and $\Delta\Delta G$ are different metrics, it is expected that deleterious mutations, on average, should have a higher impact on protein structure that benign mutations. Therefore, accurate $\Delta\Delta G$ predictions should have a higher correlation with the deleteriousness score, defined as 1 for deleterious mutations and 0 for benign mutations.

The performance on all datasets is correlated.

$$\begin{aligned} combined\_score_{core} = \frac{1}{7} \cdot \Big[& 3 \cdot Cross\_validation \\ & + Humsavar + ClinVar + COSMIC \\ & + Taipale \Big] \end{aligned} \tag{3.1}$$

$$combined\_score_{interface} = \frac{1}{6.5} \cdot \Big[3 \cdot Cross\_validation + Humsavar + ClinVar + COSMIC + \frac{1}{4} \cdot (Taipale\_PPI + Taipale\_GPCA) \Big] \quad (3.2)$$

3.3 Feature elimination

3.4 Validation

We used a combined score to select the best SGB hyperparameters during grid-search over parameter space, and to select the optimal number of features during feature elimination.

SGB hyperparameters and the number of features to optimize both cross-validation performance on the training set and performance on the validation sets.

output and the validation parts of those datasets throughout hyperparameter optimization (green, red and purple lines in Figures 3.3 and 3.4) and feature elimination (green, red and purple lines in Figures 3.5 and 3.6). ELASPIC uses the stochastic gradient boosting regression (GBR) algorithm, implemented in scikit-learn [35].

ELASPIC described in output xxx features in total. 1. We calculated those features for the Provean and the Skempi training sets. 2. We removed features that were note different in any of the training cases (xxx for core mutations and yyy for interface mutations).

3. It has been reported that balancing the training set by including both positive and negative samples

As described in [], balancing the training set can significantly improve performance. However, with Provean balancing the training set can bias the result because most mutations are to unconserved amino acids (often alanine) and

Most structural features play a surprisingly small role in the performance of the ELASPIC predictor. In fact, we can achieve near-optimal performance with both core and interface predictors by using only 6 features (displayed in bold in Tables 3.5 and 3.6). This suggests either that most features are not informative in predicting the energetic effect of mutations, or that the training set is too noisy for the contribution of those features to make a significant impact on the accuracy of the predictor.

Provean score and, in the case of the core predictor, BLOSUM62 matrix score, where the only sequence-based featurs selected through feature elimination.

We built two core predictors and two interface predictors:

1. No sequence features but a balanced training set.

2. Sequence features but no balanced training set.

- Accuracy over different sequence identity bins
- within protein correlation on the test set

3.5 Datasets

3.6 Machine learning

3.7 Predicting mutation-induced changes in the Gibbs free energy of protein folding

3.7.1 Hyperparameter optimization and feature elimination

3.7.2 Validation

3.8 Predicting mutation-induced changes in the Gibbs free energy of protein-protein interaction

3.8.1 Hyperparameter optimization and feature elimination

3.8.2 Validation

Table 3.1: Description of the datasets that were used in this study.

Name	Type	Description
Protherm	Train	Database of mutations-induced changes in the Gibbs free energy of protein folding ($\Delta\Delta G_{core}$) [40].
Skempi	Train	Database of mutations-induced changes in the Gibbs free energy of protein-protein interactions ($\Delta\Delta G_{interface}$) [41].
Taipale	Validation	Interaction between chaperones and wildtype or mutant proteins, quantified using the LUMIER assay [42].
Taipale PPI	Validation	Results of yeast two-hybrid experiments, measuring the presence or absence of protein-protein interactions for wild-type and mutant proteins [42].
Taipale GPCA	Validation	*Gaussia princeps* luciferase protein complementation assay, measuring the effect of mutations on protein affinity [42].
Humsavar	Validation & Test	Disease-causing mutations and polymorphisms obtained from the UniProt *humsavar.txt* file [36]. Mutations annotated with at least one disease were assigned a value of 1. Mutations annotated as "polymorphisms" were assigned a value of 0.
ClinVar	Validation & Test	Disease-causing mutations and polymorphisms obtained from ClinVar [38]. Mutations found in the ClinVar *clinvar_20160531.vcf* file were assigned a value of 1. Mutations found in the ClinVar *common_no_known_medical_impact_20160531.vcf* file were assigned a value of 0.
COSMIC	Validation & Test	Mutations found in cancer [37]. Mutations classified by FATHMM [7] as cancer drivers were assigned a value of 1. Mutations classified by FATHMM as cancer passengers were assigned a value of 0.
SUMO Ligase	Test	Mutations affecting the activity of SUMO ligase, measured using a cell viability assey [43].
AB-Bind	Test	Mutations explored in antibody affinity maturation experiments [44].
Benedix	Test	Mutations from alanine scanning of the TEM1 (β-lactamase) – BLIP (β-lactamase-inhibitor) interface [16].

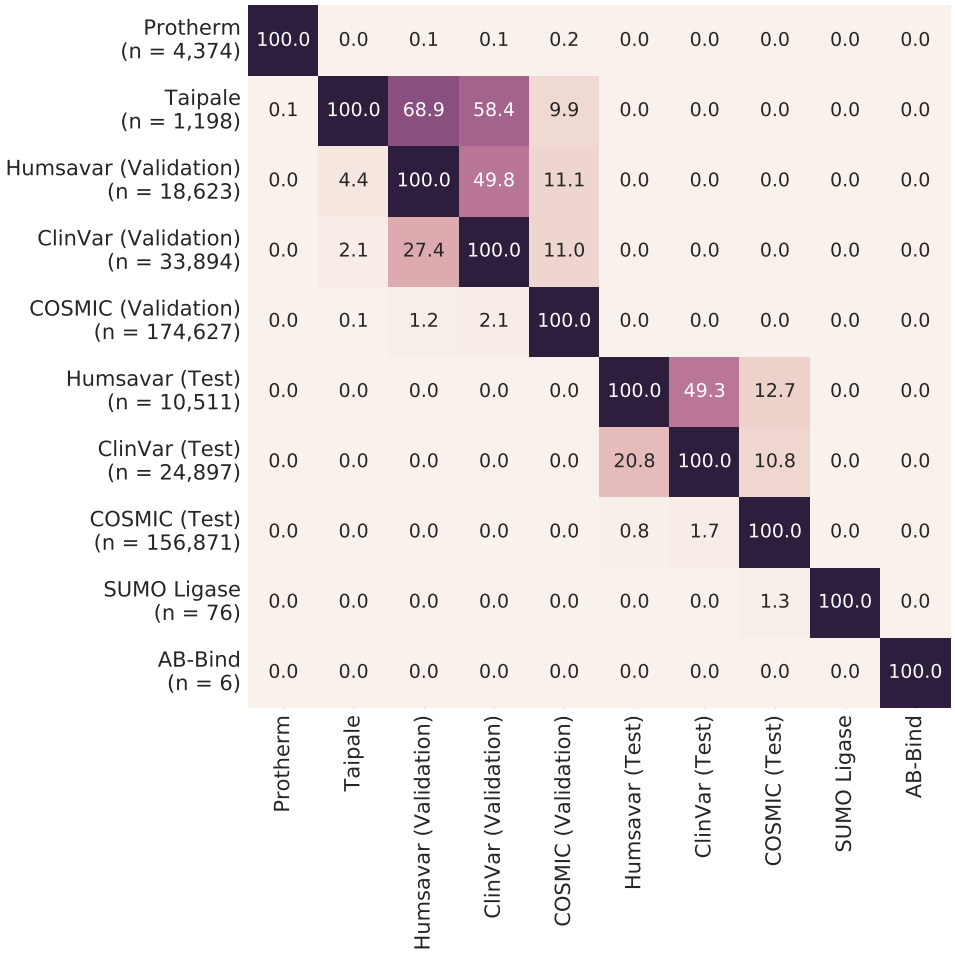

Figure 3.1: Overlap in core mutations between all the datasets used in this study. The shade and value inside each square denotes the percentage of mutations in the dataset named on the y-axis that are also found in the database named on the x-axis. Core mutations are defined as mutations that do not occur within 6 Åof a neighbouring chain in the provided PDB or protein-protein homology model. A description of each dataset can be found in Table 3.1.

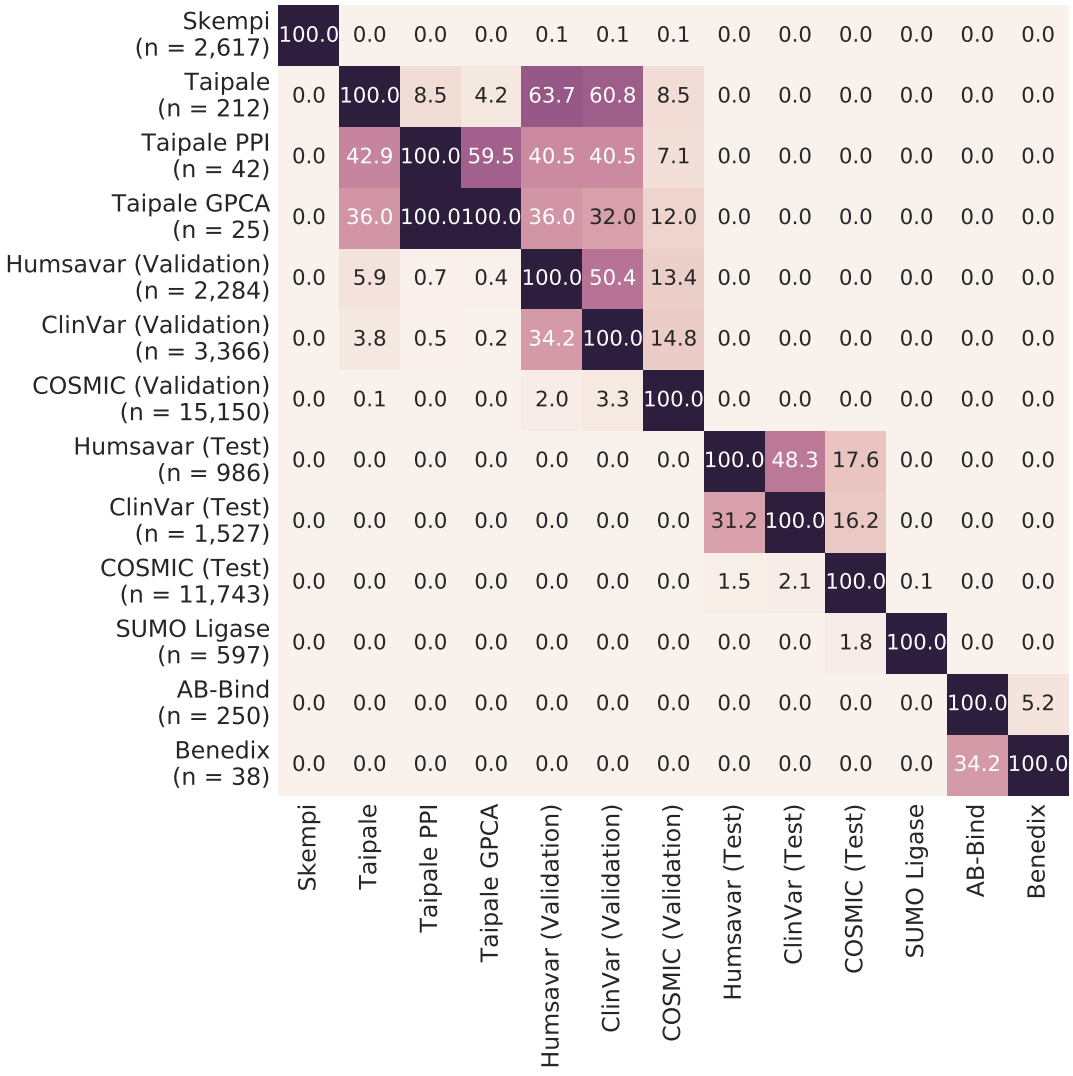

Figure 3.2: Overlap in interface mutations between all the datasets used in this study. The shade and value inside each square denotes the percentage of mutations in the dataset named on the y-axis that are also found in the database named on the x-axis. Interface mutations are defined as mutations that occur within 6 Åof a neighbouring chain in the provided PDB or protein-protein homology model. A description of each dataset can be found in Table 3.1.

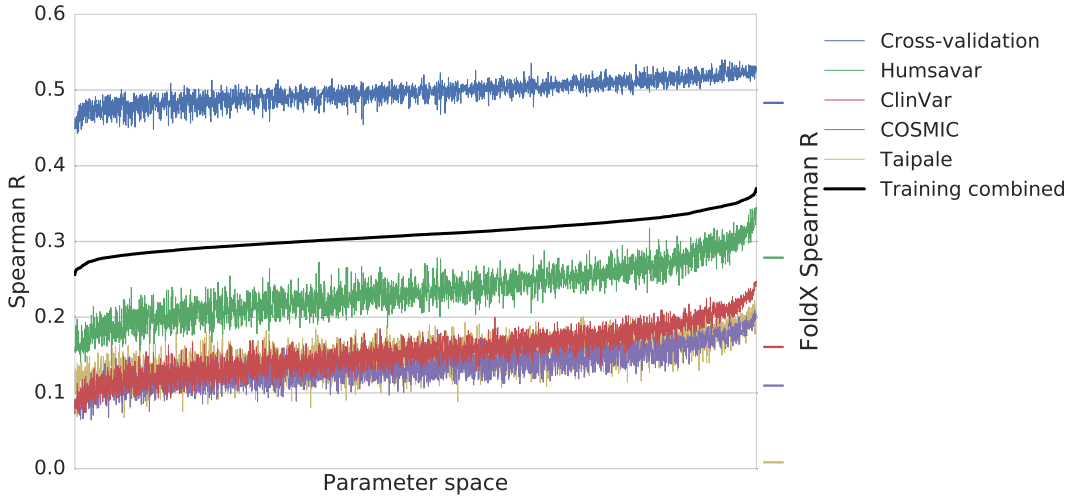

Figure 3.3: Core predictor hyperparameter optimization.

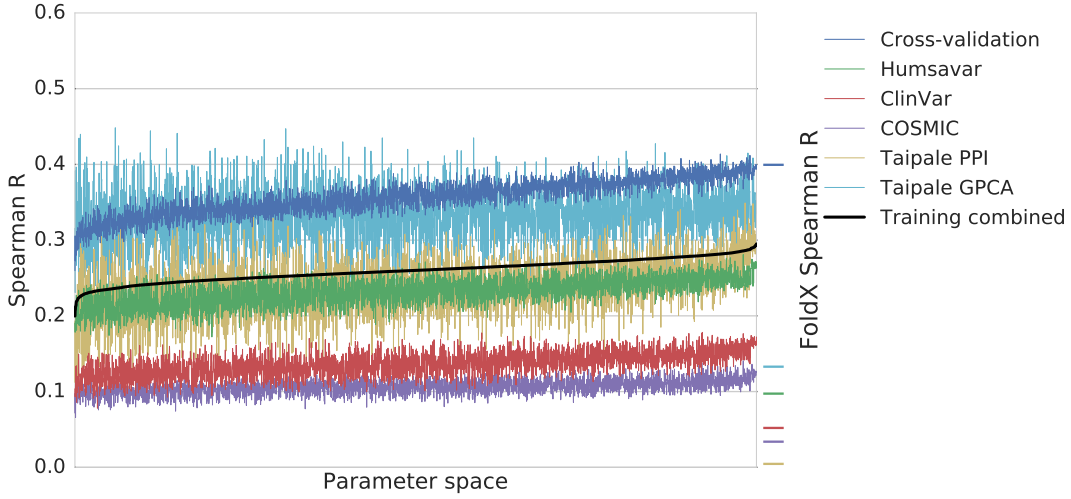

Figure 3.4: Interface predictor hyperparameter optimization.

Table 3.2: GradientBoostingRegressor evaluated through gridsearch.

Parameter name	Parameter value
alpha	0.99, 0.95, 0.9, 0.8, 0.7, 0.5
learning_rate	0.1, 0.05, 0.02, 0.01
loss	huber
max_depth	10, 8, 6, 4
max_features	1.0, 0.8, 0.5, 0.3, 0.1,
min_samples_leaf	29, 21, 17, 13, 9, 5, 3
n_estimators	2000

Table 3.3: Core predictor parameters.

Parameter name	Parameter value
alpha	0.5
learning_rate	0.01
loss	huber
max_depth	4
max_features	0.246
min_samples_leaf	17
n_estimators	2000

Table 3.4: GradientBoostingRegressor parameters selected using grid-search.

Parameter name	Parameter value
alpha	0.9
learning_rate	0.01
loss	huber
max_depth	4
max_features	0.766
min_samples_leaf	13
n_estimators	2000

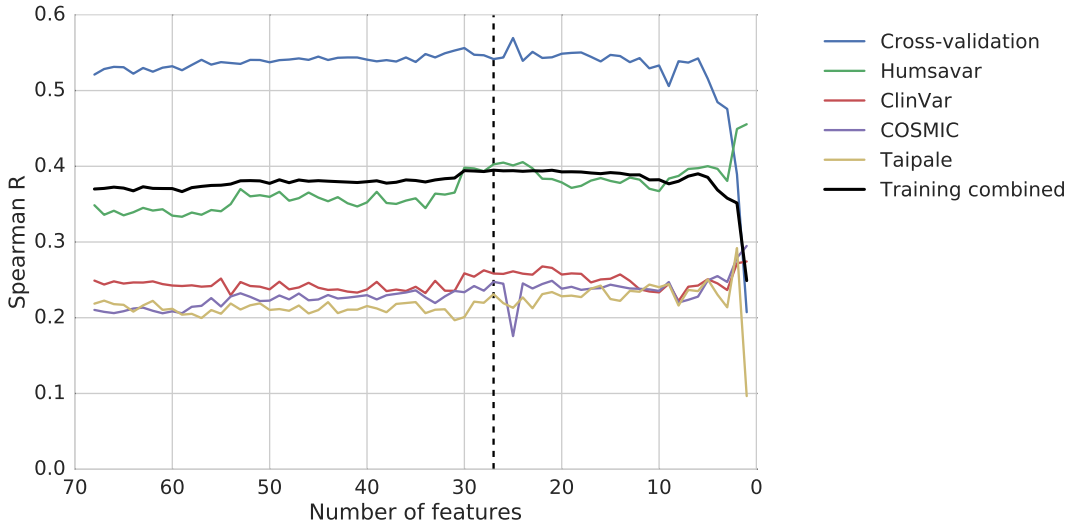

Figure 3.5: Feature elimination curve for the ELASPIC core predictor.

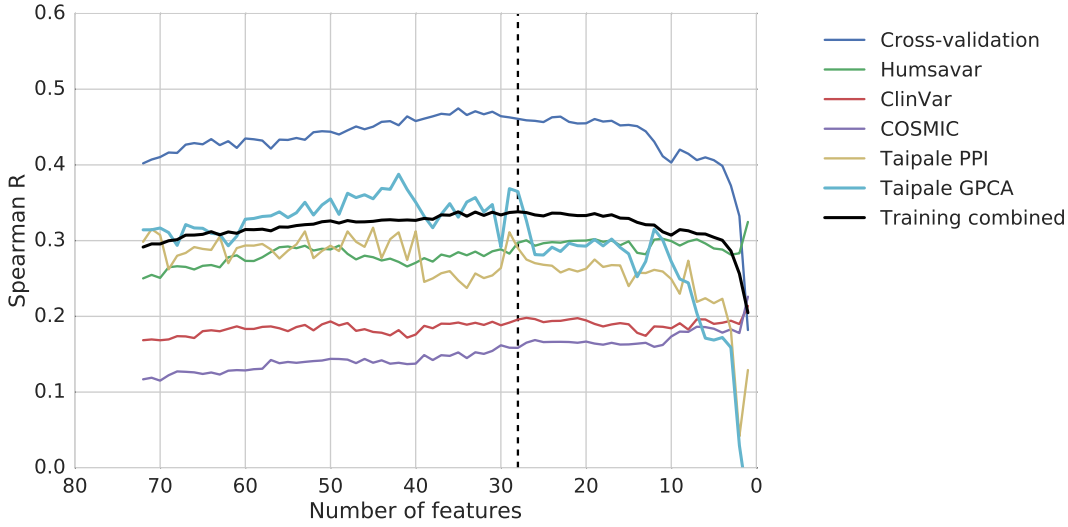

Figure 3.6: Feature elimination curve for the ELASPIC interface predictor.

Table 3.5: Core predictor features. Bold indicates the top-6 most important features. FoldX feature descriptions were taken from urlhttp://foldxsuite.crg.eu/command/Stability.

Feature name	Feature source	Feature description
alignment_coverage	ELASPIC	Structural template alignment coverage.
alignment_identity	ELASPIC	Structural template sequence identity.
alignment_score	ELASPIC	Structural template quality (Equation 2.1).
backbone_hbond_change	FoldX	Backbone hydrogen bond energy.
backbone_hbond_wt	FoldX	This the contribution of backbone hydrogen bonds.
cis_bond_wt	FoldX	Cis peptide bond energy.
disulfide_wt	FoldX	Contribution of disulfide bonds.
electrostatic_kon_change	FoldX	Electrostatic interaction between molecules in the pre-complex.
electrostatics_change	FoldX	Electrostatic interactions.
entropy_mainchain_change	FoldX	Entropy cost of fixing the main chain.
helix_dipole_wt	FoldX	Electrostatic contribution of the helix dipole.
matrix_score	ELASPIC	BLOSUM62 matrix score.
pcv_hbond_change	ELASPIC	Hydrogen-oxygen contacts involving atoms of the mutated residue and atoms of the interacting chain.
pcv_hbond_self_change	ELASPIC	Hydrogen-oxygen contacts involving atoms of the mutated residue and atoms of the mutated chain.
pcv_salt_equal_change	ELASPIC	Charge repulsions between atoms of the mutated residue and atoms of the interacting chain.
pcv_salt_equal_self_wt	ELASPIC	Charge repulsions between atoms of the mutated residue and atoms of the mutated chain.
pcv_salt_equal_wt	ELASPIC	Charge repulsions between atoms of the mutated residue and atoms of the interacting chain.
pcv_salt_opposite_change	ELASPIC	Charge attractions between atoms of the mutated residue and atoms of the interacting chain.
pcv_vdw_self_change	ELASPIC	Carbon carbon contacts between atoms of the mutated residue and atoms of the mutated chain.
provean_score	Provean	Sequence conservation score.
sloop_entropy_wt	FoldX	Entropic cost according to the SLoop database of loop conformations.
solvation_hydrophobic_change	FoldX	Contribution of hydrophobic groups.
solvation_polar_change	FoldX	Energetic penalty for burying polar groups.
solvent_accessibility_wt	MSMS	Solvent-accessible surface area of the mutated residue.
torsional_clash_change	FoldX	Intra-residue Van der Waals torsional clashes.
van_der_waals_clashes_change	FoldX	Energy penalization due to Van der Waals clashes (interresidue).
water_bridge_wt	FoldX	Contribution of water bridges.

Table 3.6: Interface predictor features. Bold indicates the top-6 most important features. FoldX feature descriptions were taken from urlhttp://foldxsuite.crg.eu/command/AnalyseComplex.

Feature name	Feature source	Feature description
alignment_score	ELASPIC	Alignment quality (Equation 2.2) .
backbone_clash_change	FoldX	Backbone-backbone Van der Waals energy.
backbone_clash_wt	FoldX	Backbone-backbone Van der Waals energy.
backbone_hbond_change	FoldX	Backbone hydrogen bond energy.
cis_bond_wt	FoldX	Cis peptide bond energy.
electrostatic_kon_wt	FoldX	Electrostatic interaction between molecules in the pre-complex.
energy_ionisation_wt	FoldX	Ionization energy.
entropy_complex_change	FoldX	Entropic cost of forming a complex.
entropy_sidechain_change	FoldX	Entropic cost of fixing the side chain.
intraclashes_energy_2_change	FoldX	Van der Waals clashes of residues at the interface of the complex with their own molecule (type 2).
partial_covalent_bonds_wt	FoldX	Interactions with bound metals.
pcv_hbond_self_change	ELASPIC	Hydrogen-oxygen contacts involving atoms of the mutated residue and atoms of the mutated chain.
pcv_hbond_wt	ELASPIC	Hydrogen-oxygen contacts involving atoms of the mutated residue and atoms of the interacting chain.
pcv_salt_equal_self_change	ELASPIC	Charge repulsions involving atoms of the mutated residue and atoms of the mutated chain.
pcv_salt_equal_wt	ELASPIC	Charge repulsions involving atoms of the mutated residue and atoms of the interacting chain.
pcv_salt_opposite_change	ELASPIC	Charge attractions involving atoms of the mutated residue and atoms of the interacting chain.
pcv_salt_opposite_self_change	ELASPIC	Charge attractions involving atoms of the mutated residue and atoms of the mutated chain.
pcv_salt_opposite_self_wt	ELASPIC	Charge attractions involving atoms of the mutated residue and atoms of the mutated chain.
pcv_vdw_self_change	ELASPIC	Carbon carbon contacts involving atoms of the mutated residue and atoms of the mutated chain.
pcv_vdw_self_wt	ELASPIC	Carbon carbon contacts involving atoms of the mutated residue and atoms of the mutated chain.
pcv_vdw_wt	ELASPIC	Carbon carbon contacts involving atoms of the mutated residue and atoms of the interacting chain.
provean_score	Provean	Sequence conservation score.
sloop_entropy_change	FoldX	Entropic cost according to the SLoop database of loop conformations.
solvation_hydrophobic_change	FoldX	Contribution of hydrophobic groups.
solvation_polar_change	FoldX	Energetic penalty for burying polar groups.
solvation_polar_wt	FoldX	Energetic penalty for burying polar groups.
torsional_clash_change	FoldX	Intra-residue Van der Waals torsional clashes.
water_bridge_change	FoldX	Contribution of water bridges.

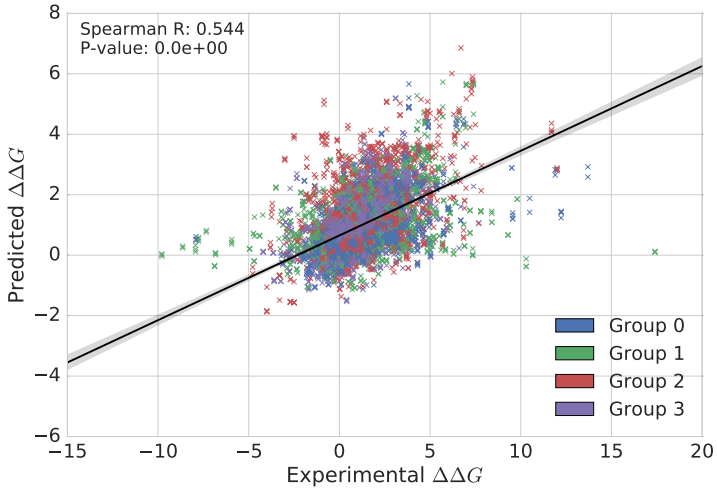

(a) Four-fold cross-validation performance on the training dataset. Colors indicate cross-validation bins.

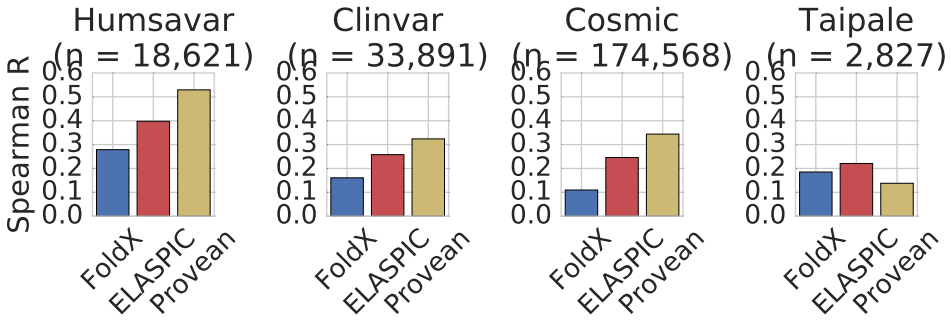

(b) Performance on the validation datasets.

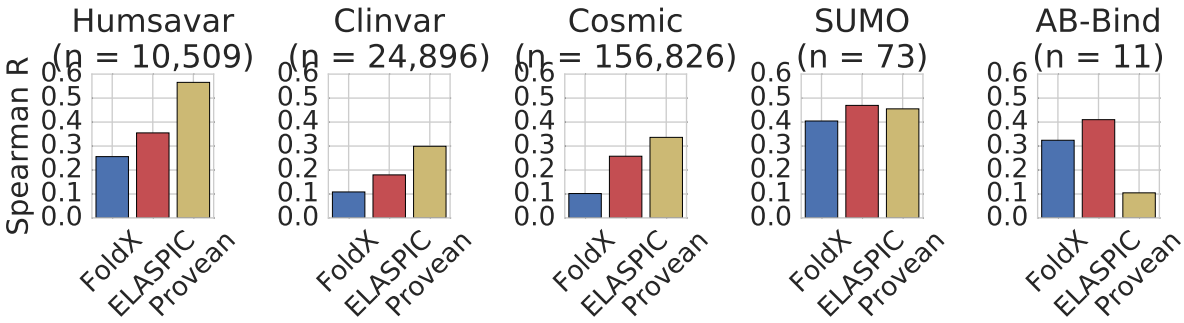

(c) Performance on the test datasets.

Figure 3.7: Performance of the core predictor on the training (a), validation (b) and test sets (c).

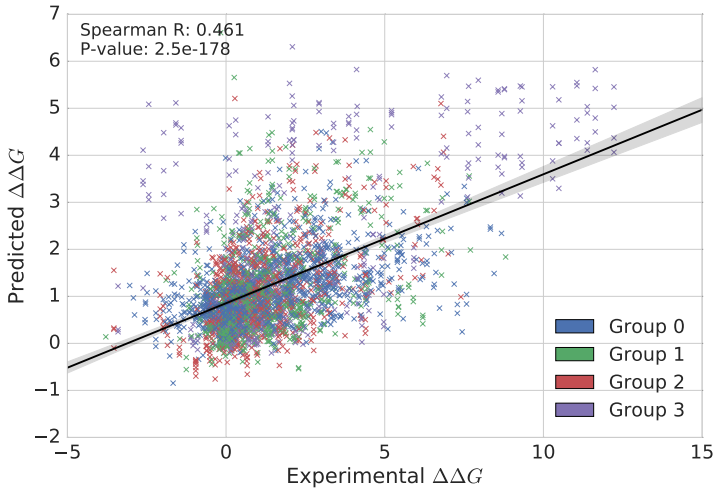

(a) Four-fold cross-validation performance on the training dataset. Colors indicate cross-validation bins.

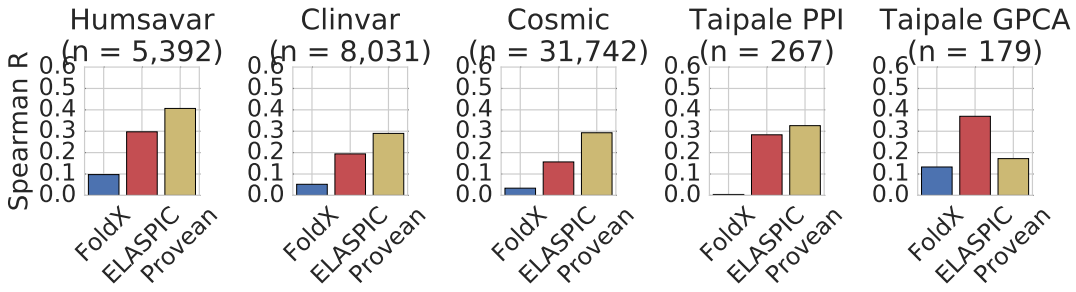

(b) Performance on the validation datasets.

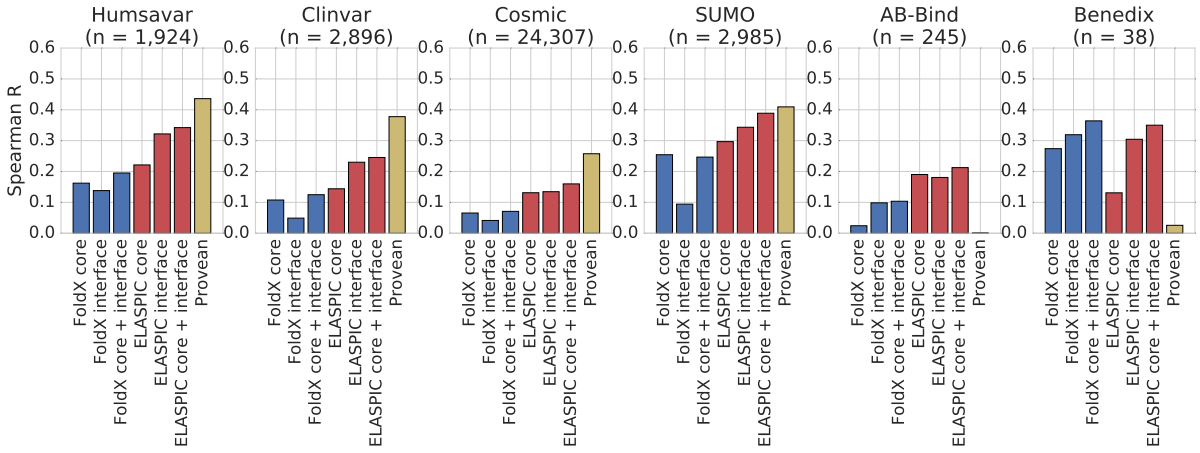

(c) Performance on the test datasets.

Figure 3.8: Performance of the interface predictor on the training (a), validation (b) and test sets (c).

Chapter 4

Discussion

In the set of features selected through feature elimination, there are both sequence-based features and structure-based features. The most important sequence-based feature is the Provean score

Out of the remaining featues, Results of feature elimination support the view that electrostatics, Van der Waals forces and entropy are the main forces determining the effect of mutations, as proposed by Benedix *et al.* in the Concoord/Poisson-Boltzmann surface area model (Equation 4.1).

Out of the features that remain after feature elimination.

$$\Delta G_{CC/PBSA} = \Delta G_{electrostatic} + \Delta G_{van\ der\ Waals} + \Delta G_{entropy} \tag{4.1}$$

"By weighting the individual averaged energy contributions (sepa- rately for folding free energies and protein-protein binding affinities) water contributions are implicitly taken into account."

- Use covariation between amino acids in addition to the conservation score to predict the impact of mutations, as described by Kowarsch et. al. [45].

- Standard conservation metrics, such as Provean, may predict a certain substitution to be benign because it occurs in other organisms. However, this does not take into account any potentially covarying mutations that mask the deleterious effect of the mutation in question.

- Use multiple templates when building the homology models. - Create multiple models and choose the one with the highest DOPE score. - Refine the model using molecular dynamics, although it has been reported that long-term MD is not useful for optimizing structures in most cases [46].

Cystic fibrosis

Long QT syndrome

- Assessment of the predictive accuracy of five *in-silico* prediction tools, alone or in combination, and two meta-servers to classify long QT syndrome gene mutations.

- `http://www.ncbi.nlm.nih.gov/pubmed/25967940`

Since the publication of the ELASPIC pipeline [22] and webserver [25], several other algorithms have been published which use a similar approach as ELASPIC to either predict mutation deleteriousness [47] or the $\Delta\Delta G$.

VIPUR [47]

MutaBind [48].

4.1 Protein science

Chapter 5

Future directions

5.1 Better features

Most structural features play a surprisingly small role in the performance of the ELASPIC predictor. Either those features are not informative, or the training set is too noisy for their contribution to make a significant impact on predictor accuracy.

- Use covariation between amino acids in addition tho the conservation score to predict the impact of mutations, as described by Kowarsch et. al. [45].
- Standard conservation metrics, such as Provean, may predict a certain substitution to be benign because it occurs in other organisms. However, this does not take into account any potentially covarying mutations that mask the deleterious effect of the mutation in question.

- Use multiple templates when building the homology models.
- Create multiple models and choose the one with the highest DOPE score.
- Refine the model using molecular dynamics.

Long-term MD is not useful for optimizing structures in most cases [46].

5.1.1 Multitask learning

Construct a shared representation for related problems in order to

In this work, we attempted to improve the performance of ELASPIC by keeping track of its performance on mutation deleteriousness datasets throughout cross-validation and feature selection. While this approach should prevent us from selecting a predictor which is over-fitted on the training dataset, it does not improve the pool of predictors from which we make this selection.

One way in which we could use information from the mutation deleteriousness datasets directly in the ELASPIC predictor is by training a boosted decision tree model to predict the mutation deleteriousness score, and using the output of the trained model as input to logistic regression which is trained to predict the $\Delta\Delta G$ of mutations. A similar approach was used successfully by a group at Facebook to predict clicks on adds [49]. This approach would have an additional advantage, in that since we use a linear model to predict the final $\Delta\Delta G$, it should be able to extrapolate outside the values present in our training set.

An additional advantage is that the feature learning part of the predictor would be done on a much larger dataset, allowing the sequential and structural features to "mix" in a more general environment.

"The resulting transformer has then learned a supervised, sparse, high-dimensional categorical embedding of the data."

5.2 Multi-residue mutations

ELASPIC can easily be extended to calculate the $\Delta\Delta G$ for mutations involving multiple amino acids. The tricky part is that the number of features changes with the number of amino acids that are mutated. We could address this by treating a mutation affecting multiple amino acids as a set of single amino acid mutations. For example, we could use the following recursive strategy:

1. Introdue each of the single amino acid mutations, one at a time.
2. Select the single amino acid mutation with the most stabilizing effect.
3. Repeat for the remaining mutations, using the structure containing the mutation selected in Step 2.

About one third on mutations in the Protherm and Skempi databases affect multiple amino acids. We could include those mutations in the training set by dividing them into single amino acid mutations and assigning to them a $\Delta\Delta G$ proportional to their contribution to the overall mutation score, as determined by the multiple amino acid substitution version of ELASPIC. This would require "bootstrapping" the ELASPIC predictor using single amin acid mutations, using the "bootstrapped" predictor to approximate the contribution of single amino acid mutaitons to the $\Delta\Delta G$ affecting mulitple amino acids, adding those mutations to the training set, and repeating.

In the case of the ELASPIC core predictor, we could create a dataset of multiple amino acid polymorphisms (MAAMs) from a thermophilic bacterium and it's closest non-thermophilic relative (maybe such a database already exists?). Cross-validate ELASPIC making sure that we predict those MAAMs to be stabilizing. Incorporate those MAAMs into our training set, weighting them accordingly.

In the case of the ELASPIC interface predictor, we could construct a dataset from phage-display read counts, and cross-validate ELASPIC while keeping track of its performance on phage display counts. Could then recursively incorporate the phage display data into the training set, weighting it by how well the ELASPIC predictor does on those mutations, as determined through cross-validation.

It is likely that the performance of the ELASPIC predictor would be lower for mutations affecting multiple amino acids than for mutations affecting a single amino acids, as the former is more likely to induce changes in the conformation of the protein that are not modelled by ELASPIC. This drop in performance could in-part be ameliorated by including a backbone relaxation step between each mutation, using molecular dynamics [50], Rosetta Backrub [51], or other algorithms [52].

If the ELASPIC predictor can achieve reasonable results for mutations affecting multiple amino acids, it could be used "in reverse" to design protein domains with increased stability and protein interfaces with increased affinity.

FireProt: Energy- and Evolution-Based Computational Design of Thermostable Multiple-Point Mutants

- `http://journals.plos.org/ploscompbiol/article?id=10.1371%2Fjournal.pcbi.1004556`

- Predict the structural effect of multiple mutations.

- “Stability effects of all possible single-point mutations were estimated using the ¡BuildModel¿ module of FoldX”.

- We demonstrate that thermostability of the model enzymes haloalkane dehalogenase DhaA and -hexachlorocyclohexane dehydrochlorinase LinA can be substantially increased.

- [53]

HOPE THAT PROVEAN WOULD AT LEAST PARTIALLY MAKE UP FOR THE LIMITING ASSUMPTION THAT THE BACKBONE REMAINS STABLE BETWEEN MUTATIONS.

SCIENTIFICALLY INTERESTING TO SEE WHAT EFFECT MD RELAXATIONS WOULD HAVE ON THE PERFORMANCE OF THE ALGORITHM.

5.3 Additional interaction types

5.3.1 Protein-protein interactions

Predict PPIs: PRISM: Protein interaction by structure matching.

5.3.2 Protein-ligand interactions

- drugging protein-protein interfaces [54]

Platinum: Protein-ligand affinity change upon mutation database.

- `http://bleoberis.bioc.cam.ac.uk/platinum/`

BioLiP is a semi-manually curated database for high-quality, biologically relevant ligand-protein binding interactions.

- `http://zhanglab.ccmb.med.umich.edu/BioLiP/`

- The structure data are collected primarily from the Protein Data Bank, with biological insights mined from literature and other specific databases.

5.3.3 Protein-DNA/RNA interactions

ProNIT

RBPDB: a database of RNA-binding specificities

`http://rbpdb.ccbr.utoronto.ca`

Paper: `http://nar.oxfordjournals.org/content/39/suppl_1/D301`

5.3.4 Protein-peptide interactions

ELM

5.3.5 Phosphorylated residue-mediated interactions

5.4 ELASPIC v2.0

eSCOP

Gene3D

- Use sequence profiles (e.g. Pfam or Gene3D) to guide the alignment.

Bibliography

[1] KA. Wetterstrand. *DNA Sequencing Costs: Data from the NHGRI Genome Sequencing Program (GSP).* May 24, 2016.

[2] Caitlin C. Chrystoja and Eleftherios P. Diamandis. "Whole Genome Sequencing as a Diagnostic Test: Challenges and Opportunities". In: *Clinical Chemistry* 60.5 (May 2014), pp. 724–733. DOI: 10.1373/clinchem.2013.209213.

[3] Serena Nik-Zainal et al. "Landscape of Somatic Mutations in 560 Breast Cancer Whole-Genome Sequences". In: *Nature* 534.7605 (June 2, 2016), pp. 47–54. DOI: 10.1038/nature17676.

[4] Pauline C. Ng and Steven Henikoff. "SIFT: Predicting Amino Acid Changes that Affect Protein Function". In: *Nucleic Acids Research* 31.13 (July 1, 2003), pp. 3812–3814.

[5] Yongwook Choi et al. "Predicting the Functional Effect of Amino Acid Substitutions and Indels". In: *PLoS ONE* 7.10 (October 8, 2012). 00256, e46688. DOI: 10.1371/journal.pone.0046688.

[6] Ivan Adzhubei et al. "Predicting Functional Effect of Human Missense Mutations Using PolyPhen-2". In: *Current Protocols in Human Genetics*. John Wiley & Sons, Inc., 2001.

[7] Hashem A. Shihab et al. "Ranking Non-Synonymous Single Nucleotide Polymorphisms Based on Disease Concepts". In: *Human Genomics* 8.1 (June 30, 2014). 00000, p. 11. DOI: 10.1186/1479-7364-8-11.

[8] Biao Li et al. "Automated Inference of Molecular Mechanisms of Disease from Amino Acid Substitutions". In: *Bioinformatics* 25.21 (January 11, 2009), pp. 2744–2750. DOI: 10.1093/bioinformatics/btp528.

[9] The Cancer Genome Atlas Research Network. "Integrated Genomic Analyses of Ovarian Carcinoma". In: *Nature* 474.7353 (June 30, 2011), pp. 609–615. DOI: 10.1038/nature10166.

[10] Martin Kircher et al. "A General Framework for Estimating the Relative Pathogenicity of Human Genetic Variants". In: *Nature Genetics* 46.3 (March 2014), pp. 310–315. DOI: 10.1038/ng.2892.

[11] R Dorfman et al. "Do Common in Silico Tools Predict the Clinical Consequences of Amino-Acid Substitutions in the CFTR Gene?" In: *Clinical Genetics* 77.5 (May 1, 2010), pp. 464–473. DOI: 10.1111/j.1399-0004.2009.01351.x.

[12] MichaelR. Shirts and DavidL. Mobley. "An Introduction to Best Practices in Free Energy Calculations". In: *Biomolecular Simulations*. Ed. by Luca Monticelli and Emppu Salonen. Methods in Molecular Biology 924. Humana Press, January 1, 2013, pp. 271–311. DOI: 10.1007/978-1-62703-017-5_11.

[13] Brett D. Welch et al. "Potent D-Peptide Inhibitors of HIV-1 Entry". In: *Proceedings of the National Academy of Sciences* 104.43 (October 23, 2007), pp. 16828–16833. DOI: 10.1073/pnas.0708109104.

[14] Douglas E. V. Pires et al. "mCSM: Predicting the Effects of Mutations in Proteins Using Graph-Based Signatures". In: *Bioinformatics* 30.3 (January 2, 2014), pp. 335–342. DOI: 10.1093/bioinformatics/btt691.

[15] Josef Laimer et al. "MAESTRO - Multi Agent Stability Prediction upon Point Mutations". In: *BMC Bioinformatics* 16 (2015), p. 116. DOI: 10.1186/s12859-015-0548-6.

[16] Alexander Benedix et al. "Predicting Free Energy Changes Using Structural Ensembles". In: *Nature Methods* 6.1 (January 2009), pp. 3–4. DOI: 10.1038/nmeth0109-3.

[17] Piero Fariselli et al. "INPS: Predicting the Impact of Non-Synonymous Variations on Protein Stability from Sequence". In: *Bioinformatics* 31.17 (January 9, 2015), pp. 2816–2821. DOI: 10.1093/bioinformatics/btv291.

[18] Marharyta Petukh et al. "Predicting Binding Free Energy Change Caused by Point Mutations with Knowledge-Modified MM/PBSA Method". In: *PLOS Comput Biol* 11.7 (July 6, 2015), e1004276. DOI: 10.1371/journal.pcbi.1004276.

[19] Shane Ó Conchúir et al. "A Web Resource for Standardized Benchmark Datasets, Metrics, and Rosetta Protocols for Macromolecular Modeling and Design". In: *PloS One* 10.9 (2015), e0130433. DOI: 10.1371/journal.pone.0130433.

[20] Vladimir Potapov et al. "Assessing Computational Methods for Predicting Protein Stability upon Mutation: Good on Average but Not in the Details". In: *Protein Engineering Design and Selection* 22.9 (January 9, 2009), pp. 553–560. DOI: 10.1093/protein/gzp030.

[21] Sofia Khan and Mauno Vihinen. "Performance of Protein Stability Predictors". In: *Human Mutation* 31.6 (June 1, 2010), pp. 675–684. DOI: 10.1002/humu.21242.

[22] Niklas Berliner et al. "Combining Structural Modeling with Ensemble Machine Learning to Accurately Predict Protein Fold Stability and Binding Affinity Effects upon Mutation". In: *PLoS ONE* 9.9 (September 22, 2014), e107353. DOI: 10.1371/journal.pone.0107353.

[23] Marco Punta et al. "The Pfam Protein Families Database". In: *Nucleic Acids Research* 40 (D1 January 1, 2012). 00002, pp. D290–D301. DOI: 10.1093/nar/gkr1065.

[24] Alison L. Cuff et al. "Extending CATH: Increasing Coverage of the Protein Structure Universe and Linking Structure with Function". In: *Nucleic Acids Research* 39 (Database issue January 2011). 00100, pp. D420–D426. DOI: 10.1093/nar/gkq1001.

[25] Daniel K. Witvliet et al. "ELASPIC Web-Server: Proteome-Wide Structure-Based Prediction of Mutation Effects on Protein Stability and Binding Affinity". In: *Bioinformatics* 32.10 (May 15, 2016), pp. 1589–1591. DOI: 10.1093/bioinformatics/btw031.

[26] Thomas Rattei et al. "SIMAP—a Comprehensive Database of Pre-Calculated Protein Sequence Similarities, Domains, Annotations and Clusters". In: *Nucleic Acids Research* 38 (suppl 1 January 1, 2010). 00031, pp. D223–D226. DOI: 10.1093/nar/gkp949.

[27] Robert C. Edgar. "MUSCLE: A Multiple Sequence Alignment Method with Reduced Time and Space Complexity". In: *BMC Bioinformatics* 5.1 (August 19, 2004). 02783, p. 113. DOI: 10.1186/1471-2105-5-113.

[28] Martin H. Schaefer et al. "HIPPIE: Integrating Protein Interaction Networks with Experiment Based Quality Scores". In: *PLoS ONE* 7.2 (February 14, 2012), e31826. DOI: 10.1371/journal.pone.0031826.

[29] Thomas Rolland et al. "A Proteome-Scale Map of the Human Interactome Network". In: *Cell* 159.5 (November 20, 2014). 00006, pp. 1212–1226. DOI: 10.1016/j.cell.2014.10.050.

[30] Jean-François Rual et al. "Towards a Proteome-Scale Map of the Human Protein–protein Interaction Network". In: *Nature* 437.7062 (October 20, 2005). 02009, pp. 1173–1178. DOI: 10.1038/nature04209.

[31] Haiyuan Yu et al. "Next-Generation Sequencing to Generate Interactome Datasets". In: *Nature Methods* 8.6 (June 2011). 00070, pp. 478–480. DOI: 10.1038/nmeth.1597.

[32] Kavitha Venkatesan et al. "An Empirical Framework for Binary Interactome Mapping". In: *Nature Methods* 6.1 (January 2009). 00427, pp. 83–90. DOI: 10.1038/nmeth.1280.

[33] Benjamin Webb and Andrej Sali. "Comparative Protein Structure Modeling Using MODELLER". In: *Current Protocols in Bioinformatics*. John Wiley & Sons, Inc., 2002.

[34] Joost Schymkowitz et al. "The FoldX Web Server: An Online Force Field". In: *Nucleic Acids Research* 33 (suppl 2 January 7, 2005), W382–W388. DOI: 10.1093/nar/gki387.

[35] F. Pedregosa et al. "Scikit-Learn: Machine Learning in Python". In: *Journal of Machine Learning Research* 12 (2011), pp. 2825–2830.

[36] The UniProt Consortium. "UniProt: A Hub for Protein Information". In: *Nucleic Acids Research* 43 (D1 January 28, 2015), pp. D204–D212. DOI: 10.1093/nar/gku989.

[37] Simon A. Forbes et al. "COSMIC: Exploring the World's Knowledge of Somatic Mutations in Human Cancer". In: *Nucleic Acids Research* 43 (D1 January 28, 2015), pp. D805–D811. DOI: 10.1093/nar/gku1075.

[38] Melissa J. Landrum et al. "ClinVar: Public Archive of Interpretations of Clinically Relevant Variants". In: *Nucleic Acids Research* 44 (D1 April 1, 2016), pp. D862–D868. DOI: 10.1093/nar/gkv1222.

[39] Hongbo Zhu et al. "NOXclass: Prediction of Protein-Protein Interaction Types". In: *BMC Bioinformatics* 7.1 (January 19, 2006), p. 27. DOI: 10.1186/1471-2105-7-27.

[40] M. D. Shaji Kumar et al. "ProTherm and ProNIT: Thermodynamic Databases for Proteins and Protein–nucleic Acid Interactions". In: *Nucleic Acids Research* 34 (suppl 1 January 1, 2006), pp. D204–D206. DOI: 10.1093/nar/gkj103.

[41] Iain H. Moal and Juan Fernández-Recio. "SKEMPI: A Structural Kinetic and Energetic Database of Mutant Protein Interactions and Its Use in Empirical Models". In: *Bioinformatics* 28.20 (October 15, 2012), pp. 2600–2607. DOI: 10.1093/bioinformatics/bts489.

[42] Nidhi Sahni et al. "Widespread Macromolecular Interaction Perturbations in Human Genetic Disorders". In: *Cell* 161.3 (April 23, 2015), pp. 647–660. DOI: 10.1016/j.cell.2015.04.013.

[43] J. Weile et al. "An Atlas of Functional Amino Acid Changes in Human SUMO and SUMO Ligase." In: (In preparation).

[44] Sarah Sirin et al. "AB-Bind: Antibody Binding Mutational Database for Computational Affinity Predictions". In: *Protein Science* 25.2 (February 1, 2016), pp. 393–409. DOI: 10.1002/pro.2829.

[45] Andreas Kowarsch et al. "Correlated Mutations: A Hallmark of Phenotypic Amino Acid Substitutions". In: *PLoS Comput Biol* 6.9 (September 16, 2010), e1000923. DOI: 10.1371/journal.pcbi.1000923.

[46] Alpan Raval et al. "Refinement of Protein Structure Homology Models via Long, All-Atom Molecular Dynamics Simulations". In: *Proteins: Structure, Function, and Bioinformatics* 80.8 (August 1, 2012), pp. 2071–2079. DOI: 10.1002/prot.24098.

[47] Evan H. Baugh et al. "Robust Classification of Protein Variation Using Structural Modelling and Large-Scale Data Integration". In: *Nucleic Acids Research* 44.6 (July 4, 2016), pp. 2501–2513. DOI: 10.1093/nar/gkw120.

[48] Minghui Li et al. "MutaBind Estimates and Interprets the Effects of Sequence Variants on Protein–protein Interactions". In: *Nucleic Acids Research* 44 (W1 August 7, 2016), W494–W501. DOI: 10.1093/nar/gkw374.

[49] Xinran He et al. "Practical Lessons from Predicting Clicks on Ads at Facebook". In: *Proceedings of the Eighth International Workshop on Data Mining for Online Advertising*. ADKDD'14. New York, NY, USA: ACM, 2014, 5:1–5:9. DOI: 10.1145/2648584.2648589.

[50] Mark James Abraham et al. "GROMACS: High Performance Molecular Simulations through Multi-Level Parallelism from Laptops to Supercomputers". In: *SoftwareX* 1–2 (September 2015), pp. 19–25. DOI: 10.1016/j.softx.2015.06.001.

[51] Colin A. Smith and Tanja Kortemme. "Predicting the Tolerated Sequences for Proteins and Protein Interfaces Using RosettaBackrub Flexible Backbone Design". In: *PLOS ONE* 6.7 (July 18, 2011), e20451. DOI: 10.1371/journal.pone.0020451.

[52] Mark G. F. Sun et al. "Protein Engineering by Highly Parallel Screening of Computationally Designed Variants". In: *Science Advances* 2.7 (July 1, 2016), e1600692. DOI: 10.1126/sciadv.1600692.

[53] David Bednar et al. "FireProt: Energy- and Evolution-Based Computational Design of Thermostable Multiple-Point Mutants". In: *PLOS Comput Biol* 11.11 (November 3, 2015), e1004556. DOI: 10.1371/journal.pcbi.1004556.

[54] James A. Wells and Christopher L. McClendon. "Reaching for High-Hanging Fruit in Drug Discovery at Protein–protein Interfaces". In: *Nature* 450.7172 (December 13, 2007), pp. 1001–1009. DOI: 10.1038/nature06526.